Synthesis and Structural Characterization of Ni-Cr Nano Ferrites by Citrate-Gel Combustion Method

Rapolu Sridhar
[1]Department of BS&H, Vignan Institute of Technology & Science,
Yadadri-Bhuvanagiri-Dist.508284, Telangana State, India.

Abstract:

Chromium substituted Nickel nano ferrites were synthesized with the chemical formula, $NiCr_XFe_{2-X}O_4$ (Where X = 0.1, 0.3, 0.5, 0.7, 0.9 and 1.0) by using citrate-gel combustion method. The structural characterization was carried out by X-ray diffraction (XRD), morphology and elemental composition of the samples were studied by Scanning Electron Microscopy (SEM) with Energy Dispersive X-ray Spectroscopy (EDS). X-ray analysis shows that the samples are single phase cubic spinel structure without any impurity peak and average crystallite size was in the range 8.5-10.5 nm. The lattice parameter, X- ray density, volume of unit cell and hopping length in A-site and B-site were calculated. The IR absorption spectra were recorded at room temperature in the range of 400 to 4000 cm^{-1}, it explain the chemical bonds in spinel ferrites and shows the characteristic peaks of ferrite sample. The observed results can be explained on the basis of composition.

Keywords: Ni-Cr nano ferrites, Citrate-Gel combustion method, XRD, SEM-EDS, FT-IR.

1. Introduction

Spinel ferrites with a general formula MFe_2O_4 where M represents a divalent metal cation such as Fe, Mn, Co, Ni, Cu, Zn and Cd. These are commercially important materials because of their interesting magnetic and electrical properties [1–2]. Among the various spinel ferrites, nickel ferrite a typical inverse spinel ferrite has been generally used in electronic devices due to their remarkably high electrical resistivity, mechanical hardness, chemical stability and low cost value [3]. Divalent or trivalent substituted nickel ferrites are extensively used as magnetic materials in a wide range of technological applications because of their low eddy current and low dielectric and magnetic losses [4].

In early years, they have been synthesized by commonly used ceramic technique. However, in recent years, many physical and chemical techniques have been developed to prepare nanosized materials. For the synthesis of nanostructured materials offer some advantages by the chemical techniques in comparison with the physical techniques concerning simplicity, energy saving and product homogeneity. Several chemical methods were developed for preparing nano ferrites, the extensively used chemical methods are electro deposition [5], sol-gel route [6], co-precipitation [7], precursor method [8], hydrothermal method [9] and reverse micelle technique [10] etc., the citrate-gel auto combustion technique has been used for the synthesis of nanosize spinel ferrites because of the low cost, simplicity, time period is very less and homogeneity of final product are included among its advantages. This method produces homogeneous and stoichiometry oxides [11] and also it presents a large on the surface area and a good sinterability in relation to powders obtained by other synthesis techniques [12-13].

The effect of substitution of Fe^{3+} by Cr^{3+} in nickel ferrite system has been reported by others [14-15]. Best of my knowledge, there are no such incorporated study has been reported in the literature on the preparation of Cr substituted nickel nano ferrites through the citrate-gel auto combustion technique. The aim of the present investigation is to synthesis the compositions $NiCr_XFe_{2-X}O_4$ (Where X=0.1,0.3,0.5,0.7,0.9 and 1.0) by citrate-gel auto combustion method [16] and present the influence of Cr^{3+} ions on the structural characterization such as X-ray analysis by XRD, morphology by SEM with EDS and FTIR studies of nickel nano ferrites.

2. Experimental procedures

Materials

The mixed Ni-Cr nano ferrite system having the compositional formula $NiCr_XFe_{2-X}O_4$ (Where X=0.1, 0.3, 0.5, 0.7, 0.9 and 1.0) were synthesized by citrate-gel auto combustion method. Analytical grade raw materials (Nickel Nitrate ($Ni(No_3)_26H_2O$), Chromium Nitrate ($Cr(NO_3)_23H_2O$), Ferric Nitrate ($Fe(NO_3)_29H_2O$), Citric Acid-Citrate ($C_6H_8O_7H_2O$) and Ammonia (NH_3)) were used to prepare the samples of the Ni-Cr nano ferrite system.

Chemical reaction

$$Ni\ (NO_3)_26H_2O+2Fe\ (NO_3)_29H_2O+\ C_6H_8O_7.H_2O \longrightarrow NiFe_2O_4+29H_2O+4N_2+6CO_2+5.5O_2$$

Material synthesis

The mixed Ni-Cr nano ferrite system having the compositional formula $NiCr_XFe_{2-X}O_4$ (Where X=0.1, 0.3, 0.5, 0.7, 0.9 and 1.0) were synthesized by citrate-gel auto combustion method and preparation method mentioned in flowchart as shown in **figure 1.**

Characterizations

The structural characterization was carried out using X-ray Diffractomerter (Bruker (Karlsruhe, Germany) D8 advanced system) with a monochromatic diffracted beam Cu K_α radiation (λ=1.5405 A^O) source between the Bragg angles 20^O to 80^O in steps of 0.04^O/Sec.

The microstructure was examined of the prepared samples using thermal field emission Scanning Electron Microscope (SEM) (Hitachi-S520, Japan) with an elemental analysis by Energy Dispersive X-ray Spectroscopy (EDS).

The absorption spectra of prepared Ni-Cr nano ferrite powders were recorded at room temperature by Fourier Transform Infrared Spectroscopy (Spectrum 100, Perkin Elmer, USA) in the range of 400-4000cm^{-1} with a resolution of 1cm^{-1} using KBr pellet method.

3. Results and Discussion:

XRD analysis

Figure 2 shows the X-ray diffraction pattern of mixed Ni-Cr nano ferrite system. It shows the crystalline phases were identified with standard reference data PDF# 862267 for Nickel ferrites ($NiFe_2O_4$) from the international centre for diffraction data (ICDD). It was observed that XRD pattern can be well indexed with peaks corresponding to cubic spinel structure such as (111), (2 2 0), (3 1 1), (4 0 0), (5 1 1), (4 4 0) and (5 3 3) the strongest reflection comes from (311) plane that indicates spinel phase and all the samples show cubic spinel structure in single phase without showing any other impurity phases [17]. From X-RD data, the other parameters such as average crystallite size, lattice constant (a), volume of the cell (V), X-ray density (d_x) and hopping length between A-site(d_A) and B-site(d_B) were calculate using standard relationships as discussed elsewhere..

The crystallite size was calculated for all prepared samples using the Scherer Formula [18] with high intensity 311 peak.

$$\text{Crystallite size } D_{hkl} = \frac{0.91\lambda}{\beta\cos\theta}$$

Where λ: The wave length of incident X-ray

β: Full Width Half Maxima (FWHM)

θ: The peak position.

The calculated crystallite size values are reported in **table 1**. From the table the average crystallite size was in the range 8.5-10.5 nm. Best of my knowledge the small size mixed Ni-Cr nano ferrites samples are possible only with the citrate-gel auto combustion method no other method has resulted the such a small size nano ferrites. By this method prepared ferrite samples phase can produce very fast at low temperature but conventional methods need to high temperatures and prolonged heating time [19].

The lattice parameter (a) of each composition was calculated by using the formula [20]

$$\text{Lattice parameter (a)} = d\sqrt{h^2+k^2+l^2}$$

Where (*hkl*) are the Miller Indices,
d is interplanner spacing.

The calculated lattice parameter values are reported in **table 1** as evident in **figure 3.** It shows the lattice parameter decreases with increasing the Cr concentration in Ni nano ferrites, it may be due to the ionic radii difference between Fe^{3+} and Cr^{3+} i.e. the large ionic radii of Fe^{3+} (0.645 Å) is replaced by low ionic radius Cr^{3+} (0.615Å) in octahedral sites [21], that means mixed Ni-Cr nano ferrite system obeys Vegard's law [22]. Decrease in lattice parameter, which may be attributed to shifting on some Fe^{3+} ions form A site to B site for higher composition. A similar behavior of lattice parameter with Cr concentration was observed by several researchers in various ferrite systems [23-24].

The volume of unit cell of each composition was calculated and reported in **table 1**. The volume of the unit cell is decreases with increasing the Cr concentration in Ni nano ferrite because of the lattice parameter decreases.

The X-ray density (d_x) was calculated from the value of lattice parameter using the formula [25]

$$X-\text{ray density } d_x = \frac{8M}{Na^3} \text{ gram/cc}$$

Where 8 represents the number of molecules in a unit cell of spinel lattice
M is the molecular weight of composition
N is the Avogadro's number a is lattices parameter

Measured X-ray density values are reported in **table 1** as evident in **figure 4**. It shows that the X-ray density increases with increasing the Cr concentration in Ni nano ferrite system, which means it shows the densification of the material. The X-ray density is to dependent on the lattice parameter and molecular weight of the sample, so the Cr^{+3} concentration increase the lattice parameter decreases hence the X-ray density increases. It may be due to greater atomic weight of Fe (55.847 gm/mole) compare with atomic weight of Cr (51.996 gm/mole).

The distance between magnetic ions on B and A sites were calculated using the following relations [26].

Hopping length in A site $d_A = 0.25a\sqrt{3}$
Hopping length in B site $d_B = 0.25a\sqrt{2}$

The hopping length measured values for tetrahedral (d_A) and octahedral (d_B) sites are listed in **table 1** as evident in **figure 5**. It is clear that the distance between the magnetic ions decreases as the Cr^{+3} concentration increases. It may be explained that Cr^{3+} ion (0.615A^O) has smaller radius than Fe^{3+} ion (0.645A^O), which makes the magnetic ions become closer to each other and decreasing the hopping length. This observation is in good agreement with other researcher reports [27-28].

Microstructure and surface morphology by SEM

The images were taken at different magnifications to study the microstructure of mixed $NiCr_XFe_{2-X}O_4$ (Where X=0.1, 0.3, 0.5, 0.7, 0.9 and 1.0) nano ferrite system by Scanning Electron Microscope (SEM) as evident in **figure 6(a-f).** It shows the microstructure images of various compositions that the morphology of the particles is similar. The prepared samples are in nano scale with homogeneous broader grain size distribution. They reveal largely agglomerated, because they experience a permanent magnetic moment proportional to their volume [29]. The particle of the sample having sharpness is more or less spherical with agglomeration between the particles and a narrow size distribution.

Elemental analysis by EDS Pattern

The elemental% and atomic% of various Cr concentrations Ni nano ferrites were listed in **table 2** as evident from **figure 6(a-f)**. It shows the EDS pattern obtained for mixed $NiCr_XFe_{2-X}O_4$ (Where X=0.1, 0.3, 0.5, 0.7, 0.9 and 1.0) which gives the elemental and atomic composition in the samples. The compositions show the presence of Ni, Cr, Fe and O without precipitating cations.

FT-IR spectral analysis

The FTIR spectra of the mixed $NiCr_XFe_{2-X}O_4$ nano ferrite system (Where X=0.1, 0.3, 0.5, 0.7 and 1.0) were recorded in the range of 400 – 4000 cm^{-1} at room temperature shown in the **figure 7**. It shows the two prominent absorption bands ν_1 and ν_2 corresponding to the stretching vibration of the tetrahedral (A-site) and octahedral (B-site) around 600 cm^{-1} and 400 cm^{-1} respectively. These absorption bands represent the spinel ferrites in single phase [30] and the absorption band results are reported in **table 1**. It is clear that the vibrational spectra of ferrites characteristic the high frequency band (ν_1) lies in the range of 591to 607 cm^{-1} corresponds to Fe^{+3}-O^{-2} vibrations in tetrahedral (A site) and low frequency band (ν_2) lies in the range 472 to 492 cm^{-1} corresponds to M^{+2}-O^{-2} vibrations in octahedral sites (B site) [31]. The difference between A site and B site is due to the change in bond length of Fe^{+3}-O^{-2} at the octahedral and tetrahedral sites [32]. The bands around 3400cm^{-1}, 2400 cm^{-1} and 1600cm^{-1} are the contribution of the stretching vibration of free and absorbed water, indicated the removal of the -OH, -CO and -NO groups. Similar trend have been observed by several researchers for the Cr substitution nano ferrite systems [33-34].

4. Conclusion

The Citrate-gel auto combustion technique is to be a convenient and versatile for obtaining homogeneous nanostructured mixed Ni-Cr ferrites. X-ray diffraction confirms the formation of single phased cubic spinel structure without any impurity peak. The lattice parameter, volume of the unit cell, distance between magnetic ions was found to decrease and X-ray density increases with increase in Cr substitution in the mixed Ni-Cr nano ferrite system. SEM micrographs shows well defined nano particles of the sample powder with homogeneous broader grain size distribution. EDS spectra show the presence of Ni, Cr, Fe and O only without precipitating cations. FTIR absorption spectra revealed the presence of two significant absorption bands υ_1 and υ_2 around 600 cm^{-1} and 400 cm^{-1} characteristic of spinel ferrite. This confirms the formation of single phase spinel structure with two sub-lattices tetrahedral (A) site and octahedral (B) site.

Acknowledgements

The author grateful to Head, Department of Physics, Osmania University, Hyderabad for provided the facility to synthesis of samples.

References

[1] Chinnasamy, C.N., Narayanasamy, A., Ponpandian, N., Chattopadhyay, K., Furubayashi, T., Nakatani, I.: Phys. Rev. B 63, 184108, **2001**

[2] Harris, V.G. et al.: *J. Magn. Magn. Mater.* 321, 2035–2047, **2009**

[3] Smit, J., Wijn, H.P.J.: Ferrites. Philips Technical Library, The Netherlands, **1959**

[4] Visuanathan, B., Murthy, V.R.K.: Ferrites Materials Science and Technology. Narosa Publishing House, New Delhi, India, **1990**

[5] U. Erb, "Electrodeposited Nanocrystals: *Nanostructured Mate- rials*, Vol. 6, No. 5, **1995**, pp. 533-538.

[6] A. Chatterjee, D. Das, S. K. Pradhan and D. Chakravarty, *J. Magn. Magn. Mater.* Vol. 127, No. 1-2, **1993**.

[7] M. Pal and D. Chakravorty, Nanocrystalline Magnetic Alloys and Ceramics, Vol. 28, No. 1-2, **2003**, pp. 283-297.

[8] C. Caizer and M. Stefanescu, *Journal of Physics D*: *Applied Physics*, Vol. 35, No. 23, **2002**, pp. 3035-3040.

[9] A. Dias, *Materials Research Bulletin*, Vol. 35, No. 9, **2000**, pp. 1439- 1446.

[10] S. Gubbala, H. Nathani, K. Koizol and R. D. K. Misra, *Physica B*, Vol. 348, No. 1-4, **2004**, pp. 317- 328.

[11] S. Vivekanandhan, M. Venkateshwarlu and N. Satyanarayana, *Journal of Alloys and Compounds*, Vol. 462, No. 1-2, **2008**, pp. 328-334.

[12] K. Rama Krishna; D. Ravinder; K. Vijaya Kumar; Ch. Abraham Lincon,

World J. condens. Matter Phy. **2012**, *2*, 153
[13] Y. Wu, Y. He, T. Wu, T. Chen, W. Weng and H. Wan,
Materials Letters, Vol. 61, No. 14-15, **2007**, pp. 3174- 3178.
[14] S.H. Lee, S.J. Yoon, G.J. Lee, H.S. Kim, C.H. Yo, K. Ahn, D.H. Lee,
Mater. Chem. Phys. 61, **1999**, 147.
[15] A.M. Gismelseed, A.A. Yousif, Physica B 370 2005 215.
[16] Rapolu Sridhar, Dachepalli Ravinder, K. Vijaya Kumar
Advances in Materials Physics and Chemistry, **2012**, 2, 192-199
[17] Devan, R.S., Kolekar, Y.D., Chougule, B.K.:
J. Phys., Condens. Matter 18, 9809–9821, **2006**
[18] B. D. Cullity, "Elements of X-Ray Diffraction," Addition Wesley, Boston, **1959**, p. 132.
[19] R. G. Gupta and R. G. Mendiratta,
Journal of Applied Physics, Vol. 48, No. 2, **1977**, pp. 845-848.
[20] B. P. Ladgaonkar, P. P. Bakare, S. R. Sainkar and A. S. Vaingankar,
Materials Chemistry and Physics, Vol. 69, No. 1-3, **2001**, pp. 19-24.
[21] R.D. Shannon, Acta Crystallogr. Sect. A 32, **1976**, 751.
[22] L. Vergard, *Zeitschrift für Physik A*: *Hadrons and Nuclei*, Vol. 5, No. 1, **1921**, pp. 17-26.
[23] Sonal Singhal, Journal of Solid State Chemistry 180, **2007**, 296–300
[24] R. Arulmurugan, B. Jeyadevan, G. Vaidyanathan and S. Sendhilnathan,
J. Magn. Magn. Mater. 288, **2005**, 470.
[25] R. C. Kumbale. P. A. Shaikh, S. S. Kamble and Y. D. Kolekar,
Journal of Alloys and Compounds, Vol. 478, No. 1-2, **2009**, pp. 599-603.
[26] B. Viswanathan , V. R. K. Murthy, "Ferrite Materials Science and Technology,"
Narosa Publishing House, New Delhi, **1990**.
[27] M.A. Gabal, Y.M.A. Angari, *Materials Chemistry and Physics* 118, **2009**, 153–160
[28] A.M. Gismelseed, A.A. Yousif, Physica B 370, **2005**, 215–222
[29] Suryawanshi. S.S, Deshpand. V Sawantn. S.R, J. Mater. Chem. Phys. 59, **1999,** 199.
[30] R.M. Mohamed, M.M. Rashad, F.A. Haraz, W. Sigmund,
J. Magn. Magn. Mater. 322, **2010**, 2058.
[31] R. D. Waldron, Phys. Rev. 99, **1955**, 1727.
[32] A.K. Ghatage, S.C. Choudhari, S.A. Patil, *J. Mater. Sci. Lett.* 15, 1548, **1996**.
[33] S.M. Patange, S.E. Shirsath, B.G. Toksha, S.S. Jadhav, S.J. Shukla, K.M. Jadhav,
Appl. Phys. A Mater. Sci. Process. A95, **2009**, 429.
[34] A.S. Elkady, S.I. Hussein, M.M. Rashad, *J. Magn. Magn. Mater*. 385, **2015**, 70.

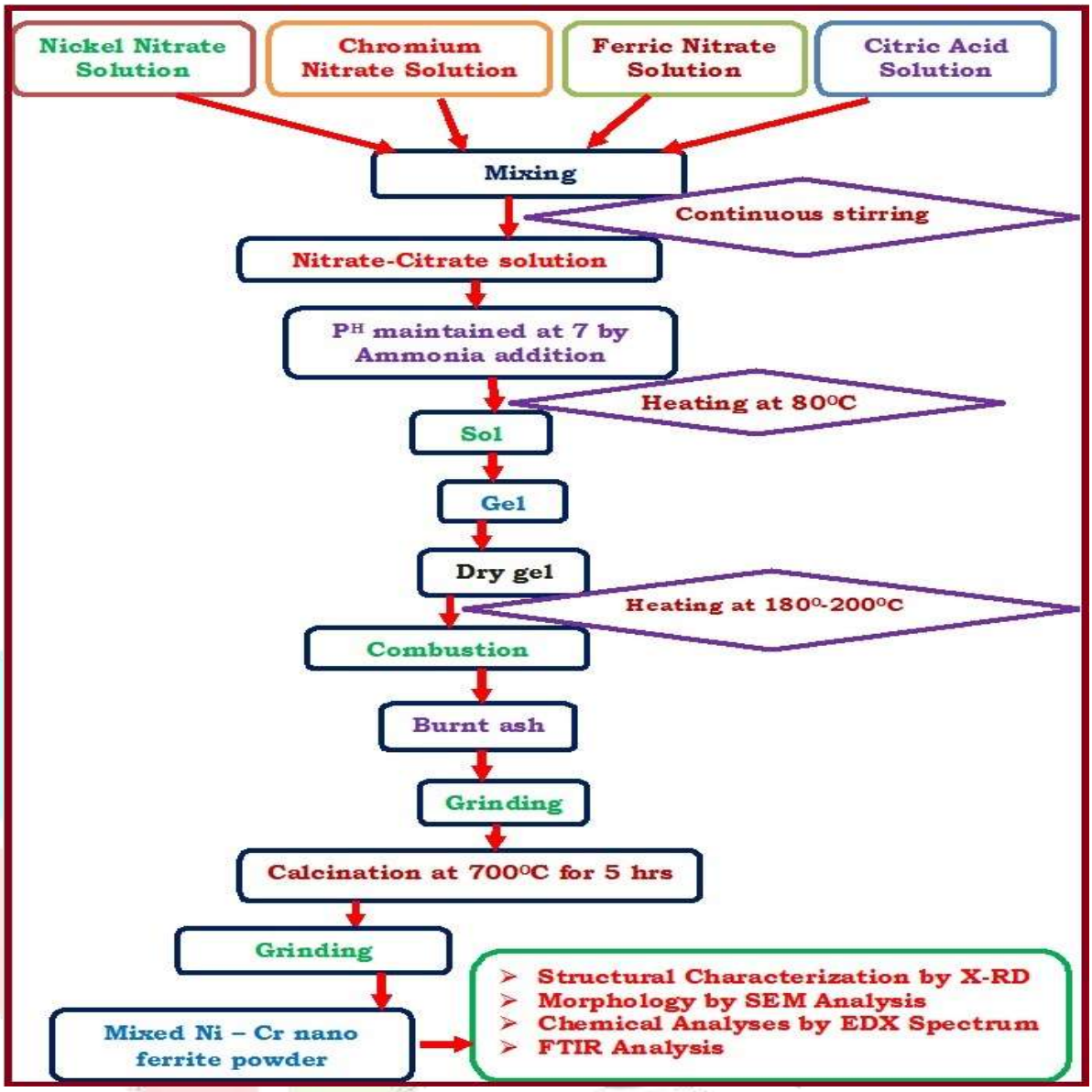

Figure 1: Flow Chart for the synthesis of mixed $NiCr_xFe_{2-x}O_4$ nano ferrite system

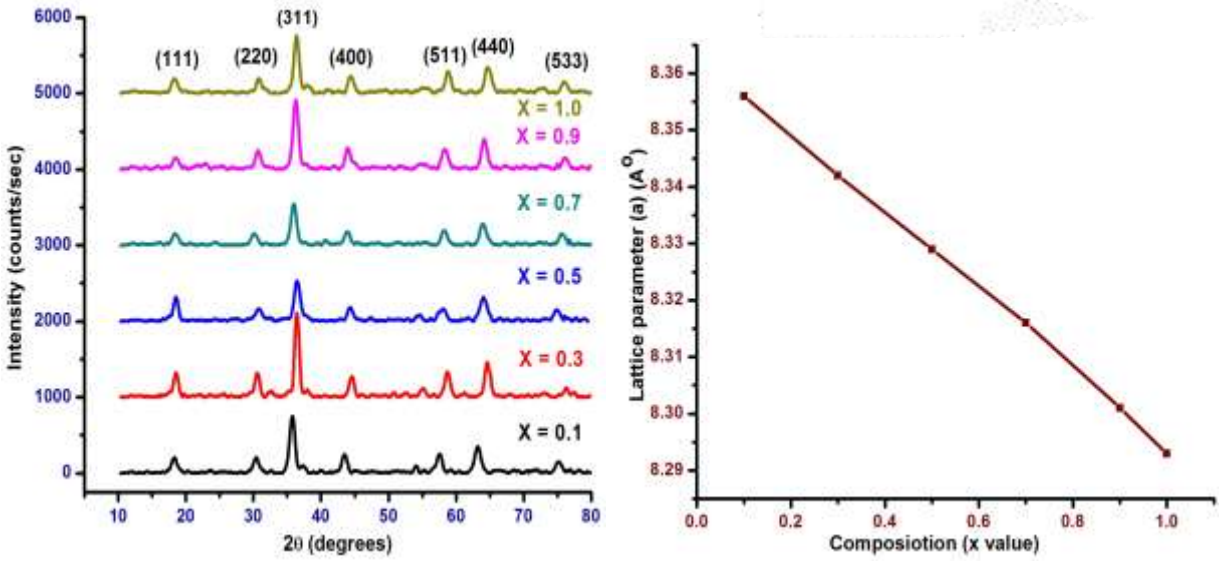

Figure 2: XRD pattern of mixed Ni-Cr nano ferrite system

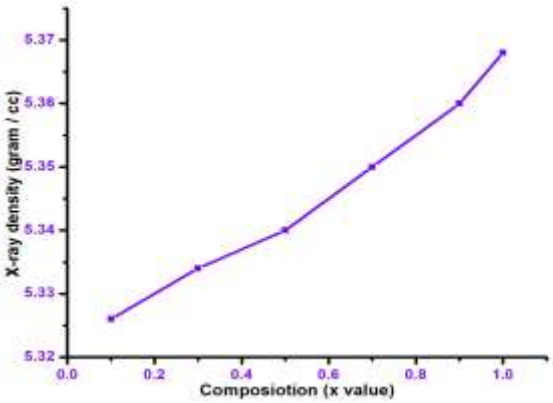

Figure 4: Variation of X-ray density with Cr concentration

Figure 3 : Variation of lattice parameter with Cr concentration

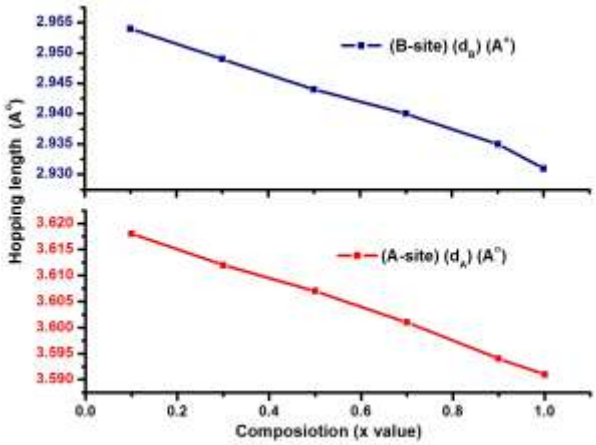

Figure 5: Variation of hopping length in A-site & B-site with Cr concentration

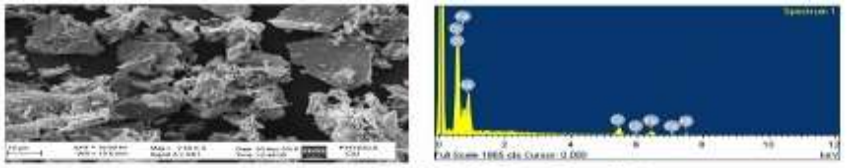

Fig. 6(a) X= 0.1 ($NiCr_{0.1}Fe_{1.9}O_4$)

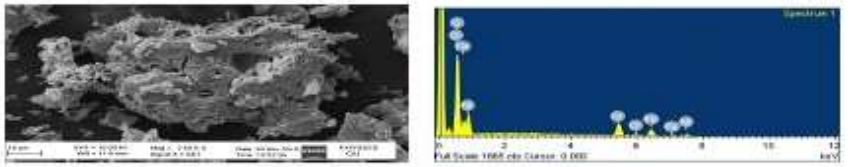

Fig. 6(b) X= 0.3 ($NiCr_{0.3}Fe_{1.7}O_4$)

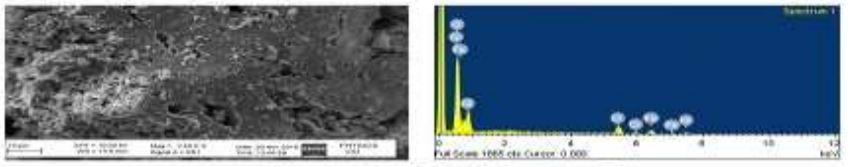

Fig. 6(c) X= 0.5 ($NiCr_{0.5}Fe_{1.5}O_4$)

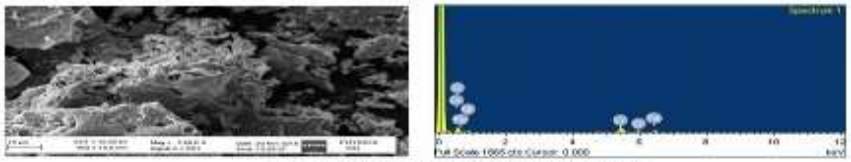

Fig. 6(d) X= 0.7 ($NiCr_{0.7}Fe_{1.3}O_4$)

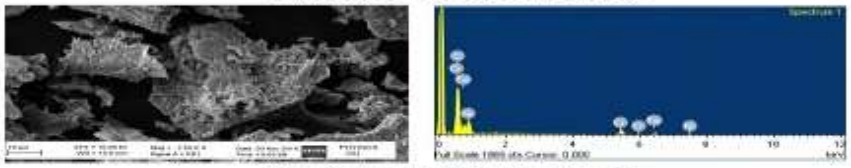

Fig. 6(e) X= 0.9 ($NiCr_{0.9}Fe_{1.1}O_4$)

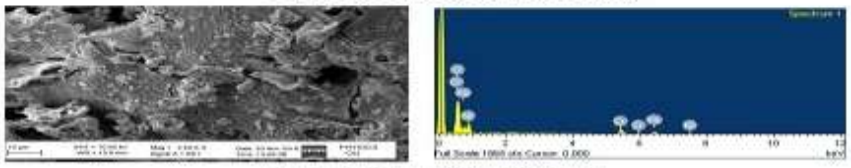

Fig. 6(f) X= 1.0 ($NiCrFe_2O_4$)

Figure 6 (a-d): SEM-EDS images of $NiCr_XFe_{2-X}O_4$ nano ferrite System

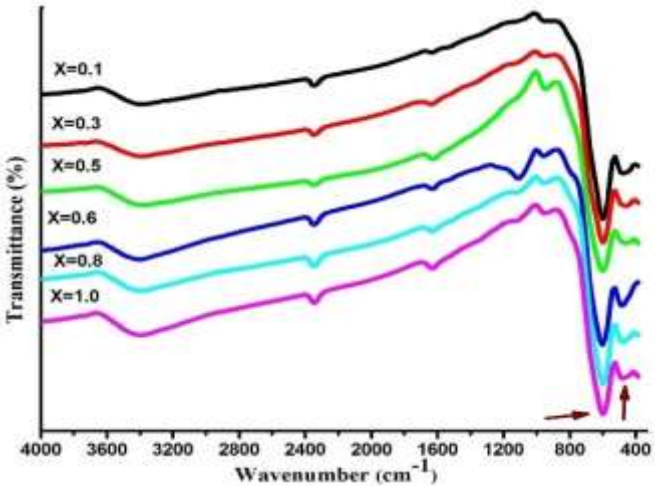

Figure 7: FTIR pattern of Mixed Ni - Cr nano ferrite system

Table – 1: XRD pattern & FTIR pattern analysis of Ni-Cr nano ferrite system

Sl.No.	Composition	Crystallite size (nm)	lattice parameter (a) (A°)	Volume of Unit Cell (V) $(A^o)^3$	X-ray density (gr/cc)	hopping length		absorption band	
						(A-site) (d_A) (A°)	(B-site) (d_B) (A°)	ν_1 (cm^{-1})	ν_2 (cm^{-2})
1	$NiCr_{0.1}Fe_{1.9}O_4$	8.96	8.356	583.485	5.33	0.408	0.333	599.96	485.35
2	$NiCr_{0.3}Fe_{1.7}O_4$	10.36	8.342	580.599	5.33	0.353	0.288	607.03	477.05
3	$NiCr_{0.5}Fe_{1.5.}O_4$	7.95	8.329	577.875	5.34	0.460	0.375	602.45	479.69
4	$NiCr_{0.7}Fe_{1.3}O_4$	8.55	8.316	575.049	5.35	0.427	0.349	591.43	481.11
5	$NiCr_{0.9}Fe_{1.1}O_4$	8.84	8.301	572.067	5.36	0.413	0.337	594.86	492.42
6	$NiCrFe_2O_4$	9.26	8.293	570.273	5.37	0.395	0.322	597.13	472.62

Table –2: Elemental analysis of each composition by EDS pattern

Element	O		Fe		Ni		Cr	
Ferrite Composition	Element %	Atomic %	Element %	Atomic %	Element %	Atomic %	Element %	Atomic %
$NiCr_{0.1}Fe_{1.9}O_4$	17.01	41.45	29.07	21.80	27.72	19.35	26.20	17.40
$NiCr_{0.3}Fe_{1.7}O_4$	19.50	45.20	29.47	21.99	25.02	16.67	26.01	16.14
$NiCr_{0.5}Fe_{1.5}O_4$	19.16	44.87	33.03	23.81	24.28	16.30	23.53	15.02
$NiCr_{0.7}Fe_{1.3}O_4$	19.79	45.86	30.76	21.96	27.30	18.14	22.15	14.04
$NiCr_{0.9}Fe_{1.1}O_4$	17.55	42.24	31.56	24.11	27.89	19.23	23.00	14.42
$NiCrFeO_4$	20.41	46.97	27.28	19.32	27.59	18.20	24.72	15.51